



**University of
Zurich**^{UZH}

**Zurich Open Repository and
Archive**

University of Zurich
University Library
Strickhofstrasse 39
CH-8057 Zurich
www.zora.uzh.ch

Year: 2017

A novel BRCA1-associated protein-1 isoform affects response of mesothelioma cells to drugs impairing BRCA1-mediated DNA repair

Parrotta, Rossella ; Okonska, Agata ; Ronner, Manuel ; Weder, Walter ; Stahel, Rolf ; Penengo, Lorenza ; Felley-Bosco, Emanuela

DOI: <https://doi.org/10.1016/j.jtho.2017.03.023>

Posted at the Zurich Open Repository and Archive, University of Zurich

ZORA URL: <https://doi.org/10.5167/uzh-136745>

Journal Article



The following work is licensed under a Creative Commons: Attribution-NonCommercial-NoDerivatives 4.0 International (CC BY-NC-ND 4.0) License.

Originally published at:

Parrotta, Rossella; Okonska, Agata; Ronner, Manuel; Weder, Walter; Stahel, Rolf; Penengo, Lorenza; Felley-Bosco, Emanuela (2017). A novel BRCA1-associated protein-1 isoform affects response of mesothelioma cells to drugs impairing BRCA1-mediated DNA repair. *Journal of Thoracic Oncology*, 12(8):1309-1319.

DOI: <https://doi.org/10.1016/j.jtho.2017.03.023>

A Novel BRCA1-Associated Protein-1 Isoform Affects Response of Mesothelioma Cells to Drugs Impairing BRCA1-Mediated DNA Repair

Rossella Parrotta, PhD,^a Agata Okonska, MSc,^a Manuel Ronner,^a Walter Weder, MD,^b Rolf Stahel, MD,^c Lorenza Penengo, PhD,^d Emanuela Felley-Bosco, PhD^{a,*}

^aLaboratory of Molecular Oncology, Division of Thoracic Surgery, University Hospital Zürich, Zürich, Switzerland

^bDivision of Thoracic Surgery, University Hospital Zürich, Zürich, Switzerland

^cCancer Center Zürich, University Hospital Zürich, Zürich, Switzerland

^dInstitute of Molecular Cancer Research, University of Zürich, Zürich, Switzerland

Received 12 September 2016; revised 8 March 2017; accepted 21 March 2017

Available online - 4 April 2017

ABSTRACT

Introduction: BRCA1 associated protein1 (BAP1) is a tumor suppressor involved in multiple cellular processes such as transcriptional regulation, chromatin modification by deubiquitinating histone 2A, and DNA repair. BAP1 mutations are frequent in malignant pleural mesothelioma (MPM). Our aim was to functionally characterize a newly identified isoform of BAP1 and investigate the effects of its expression on drug sensitivity in MPM.

Methods: Expression of BAP1 isoforms was detected by quantitative polymerase chain reaction in MPM and normal mesothelium cell lines and tumor and nontumor samples. Histone H2A ubiquitination levels were analyzed by Western blot after acidic extraction of core histones. Subcellular localization of BAP1 isoforms was examined by immunofluorescence. MPM cell survival in response to poly(adenosine diphosphate-ribose) polymerase (PARP) and dual phosphoinositide 3-kinase (PI3K)-mammalian target of rapamycin (mTOR) inhibitors was analyzed by in vitro assays.

Results: We have identified a novel alternative splice isoform of BAP1 (BAP1Δ) that misses part of the catalytic domain. Cells transfected with BAP1Δ showed reduced deubiquitinating activity compared with full-length BAP1. The expression of BAP1Δ transcript is more abundant in nontumor than in tumor samples. MPM cell lines expressing more than 20% of BAP1Δ are more sensitive to olaparib (a PARP1 inhibitor) cytotoxicity, and this sensitivity is enhanced when olaparib treatment is combined with GDC0980 (a dual PI3K-mTOR inhibitor), which induces downregulation of BRCA1.

Conclusions: These observations suggest that BAP1Δ does regulate DNA damage response and influences drug

sensitivity. It might therefore be relevant to investigate whether patients with high expression of BAP1Δ may be responsive to PARP/PI3K-mTOR inhibitors.

© 2017 International Association for the Study of Lung Cancer. Published by Elsevier Inc. This is an open access article under the CC BY-NC-ND license (<http://creativecommons.org/licenses/by-nc-nd/4.0/>).

Keywords: BRCA1 associated protein 1; Mesothelioma; PARP inhibition; BRCA1

Introduction

BRCA1-associated protein-1 (BAP1) loss-of-function mutations have been described as one of the main drivers in the complex pathogenesis of malignant pleural mesothelioma (MPM).¹⁻⁴ Germline loss of BAP1 leads to a predisposition for different types of cancer, including mesothelioma.⁵ BAP1 was initially identified in lung cancer cell lines as a protein that binds to BRCA1, DNA repair associated (BRCA1),⁶ which is a well-known

*Corresponding author.

Dr. Parrotta and Ms. Okonska equally contributed to this work.

Disclosure: The authors declare no conflict of interest.

Address for correspondence: Emanuela Felley-Bosco, PhD, Laboratory of Molecular Oncology, Thoracic Surgery, University Hospital Zürich, 8091 Zürich, Switzerland. E-mail: emanuela.felley-bosco@usz.ch

© 2017 International Association for the Study of Lung Cancer. Published by Elsevier Inc. This is an open access article under the CC BY-NC-ND license (<http://creativecommons.org/licenses/by-nc-nd/4.0/>).

ISSN: 1556-0864

<http://dx.doi.org/10.1016/j.jtho.2017.03.023>

tumor suppressor that is involved in maintenance of genomic stability and participates in DNA repair of double-strand breaks (DSBs).^{7,8} BAP1 is a 90-kDa nuclear-localized deubiquitinating enzyme with ubiquitin carboxyl hydrolase (UCH) activity, and it is the only member of the UCH family with two nuclear localization signal motifs.⁹ BAP1-mediated tumor suppression requires both deubiquitinating activity and nuclear localization of BAP1.⁹ BAP1 in a complex with the polycomb group protein additional sex combs like 1, transcriptional regulator is essential for histone 2A (H2A) deubiquitination,¹⁰ resulting in chromatin modification. BAP1 loss-of-function mutations have been described as sensitizing cancer cells to ionizing radiation and poly(adenosine diphosphate-ribose) polymerase (PARP) inhibition,^{11,12} indicating a role of functional BAP1 in promoting DSB repair.

While investigating BAP1 transcripts in MPM cell lines, we identified by serendipity a novel splice variant of BAP1 (BAP1Δ) missing part of the catalytic domain.

The expression of splice variants is not unusual in cancer because it often offers a survival advantage.¹³ We have previously described¹⁴ alternative splicing events occurring in neurofibromin 2 (NF2), another frequently mutated tumor suppressor with a driver role in this disease.^{15–19} NF2 transcripts undergo alternative splicing, generating multiple isoforms.²⁰ Isoform I, which is missing exon 16, and isoform II, which contains all 17 exons, are the two predominant species. However, only isoform I functions as a tumor suppressor and its activity is phosphorylation dependent.^{21,22} We have observed that 4% of tumor samples displayed isoform II only. Additionally, the splicing variant delE2/3, which is functionally associated with tumor development in transgenic mice if overexpressed in the absence of wild-type (WT) NF2,²³ was expressed in 35% of the MPM samples and in one sample of the inflammation and normal pleura.

In this study, our aim was to functionally characterize BAP1Δ and investigate whether its expression could be exploited for therapy.

Material and Methods

Cell Culture

The mesothelioma cell lines ZL55, ZL34, SPC111, MSTO-211H, ACC-Meso-1, and Mero8 and SDM104 normal mesothelial cells were cultured as previously described.²⁴ HEK293 cells were maintained in Dulbecco's modified Eagle's medium supplemented with 10% fetal calf serum (FCS) and 1% penicillin/streptomycin. Transfected ZL55 cells were selected with puromycin. The breast cancer cell line MCF-7 was kindly provided by Dr. Stucki (Clinic for Gynecology, University

Hospital Zürich, Zürich, Switzerland) and maintained in Roswell Park Memorial Institute medium, 10% FCS, and 1% penicillin/streptomycin. All cells were kept at 37°C in a humidified 5% CO₂ incubator.

Tumor Specimens

Tumor specimens were obtained for diagnostic purposes before chemotherapy or at the time of resection.²⁵ Normal pleural tissue was received from patients undergoing a mesothelioma-unrelated thoracic operation.²⁵ The study was approved by the University Hospital Zürich ethics committee and written informed consent was obtained from all patients. Twenty RNA samples were selected on the basis of BAP1 determined to be WT by using next-generation sequencing (Oehl and Wild, Institute of Surgical Pathology, Zürich University Hospital, manuscript in preparation) and being representative of the three MPM histologic forms: 16 of 20 epithelial (80%), three of 20 biphasic (15%), an one of 20 sarcomatoid (~1%).

Reagents

Dulbecco's modified Eagle's medium–F12 medium and penicillin/streptomycin 100x stock solution were purchased from Sigma-Aldrich Chemie GmbH (Buchs, Switzerland). Trypsin–ethylenediaminetetraacetic acid 0.25% 1× solution and Opti-MEM medium were purchased from Gibco (Life Technologies Europe, Zug, Switzerland). FCS (CVFVSF00-01) and puromycin were purchased from Eurobio (Les Ulis, France) and from AppliChem (Darmstadt, Germany), respectively. Olaparib (AZD2281, Ku-0059436) was purchased from Selleckchem (Luzern, Switzerland), and GDC-0980 was obtained from Genentech (Roche, Basel, Switzerland). DMRIE-C was purchased from Invitrogen (Carlsbad, CA).

RNA Extraction, Complementary DNA Synthesis, and Quantitative PCR

Total RNA (0.5 μg) extracted from cells, nontumoral tissue, tumors, or a pool of 12 spheroids with the RNeasy Isolation Kit (Qiagen, Hilden, Germany) was reverse-transcribed with the Quantitect Reverse Transcription Kit (Qiagen). Quantitative polymerase chain reaction (PCR) was performed as previously described.¹⁴ The primers are listed in [Supplementary Table 1](#).

Protein Extraction and Western Blotting

Total protein extracts were obtained by lysing the cells with assay buffer (Sigma Aldrich) containing 50 mM Tris-HCl, pH 8.0, with 150 mM sodium chloride, 1.0% Igepal CA-630 (NP-40), 0.5% sodium

deoxycholate, and 0.1% sodium dodecyl sulfate (SDS) supplemented with additional SDS to a final concentration of 1% and protease inhibitors, passing it through a syringe and keeping it in ice for 15 minutes. Core histones were obtained by acidic extraction as previously described.²⁶ Cytosolic and nuclear protein extracts were isolated by using the NE-PER Nuclear and Cytoplasmic Extraction Kit (Pierce Biotechnology, Waltham, MA) according to the manufacturer's instructions and nuclear versus cytosolic purity controls were assessed by probing with anti-PARP (Cell Signaling Technology, Danvers, MA) and anti-vinculin antibodies, respectively. Protein concentration was determined by using the Bradford protein assay and proteins were prepared by adding 6× reducing Laemmli buffer and boiling for 5 minutes. Five or 10 µg of total proteins or 0.5 µg of purified histones were separated on denaturing 4% to 20% gradient SDS-polyacrylamide gel electrophoresis gels, 3% to 8% gradient precast acrylamide, or 15% SDS-polyacrylamide gel electrophoresis gels depending on the target and transferred onto 0.45-µm polyvinylidene fluoride transfer membranes (Perkin Elmer, Schwerzenbach, Switzerland). The membranes were probed with the following primary antibodies: mouse anti-BAP1 (C4), rabbit anti-histone H2A, mouse anti-histone H3, mouse anti-γH2AX, mouse anti-β-actin, rabbit anti-poly(adenosine diphosphate-ribose), rabbit anti-phospho-S6 (Ser235/236), mouse anti-S6, and mouse anti-BRCA1. As a positive control for phospho-S6 (Ser235/236), cell extracts from Mero-83 cells²⁴ were used. Membranes were then incubated with the secondary antibody goat anti-mouse immunoglobulin G-horseradish peroxidase from Ancell (Bayport, MN) and goat anti-rabbit immunoglobulin G-horseradish peroxidase from Cell Signaling Technology. The signals were detected by enhanced chemiluminescence (ECL Western Blotting Reagents, GE Healthcare, Glatbrugg, Switzerland) and detected on photosensitive film (Super RX Fuji X-Ray Film, Fujifilm, Düsseldorf, Germany). Proteins were quantitated with densitometry by using Image J software, version 1.42q (National Institutes of Health, Bethesda, MD). The percentage of nuclear BAP1 was calculated in single complementary DNA (cDNA)-transfected cells as follows. Nuclear versus cytosolic BAP1, either BAP1Δ or BAP1FL, was normalized to PARP versus vinculin, respectively, and their sum was considered as total BAP1. Nuclear BAP1 was calculated as the fraction of total BAP1. In addition, because in coexpression experiments we observed the accumulation of high-molecular forms of BAP1, we quantified all the bands with a molecular weight higher than that of BAP1Δ and normalized them to PARP versus vinculin, respectively, to estimate their accumulation in the nuclear versus the cytosolic fraction.

BAP1 Cloning, Sequencing, and Transfection

Human BAP1 and BAP1Δ cDNA amplified from MPM cell lines were subcloned into the NotI site of the pCI-puro vector, which contains a puromycin resistance gene,²⁷ and inserts were validated by sequencing and deposited in Addgene (68365 and 68366, respectively). All primers are indicated in [Supplementary Table 1](#). HEK293 cells were transfected with control vector, pCI-Puro_BAP1FL, or pCI-Puro_BAP1Δ by using DMRIE-C or Lipofectamine 2000 reagent (Invitrogen) according to the manufacturer's instruction. To test the interaction between the two BAP1 isoforms, ZL55 cells stably expressing control vector or pCI-Puro_BAP1FL were transiently transfected with increasing amounts of pCI-Puro_BAP1Δ.

Clonogenic Assay

Colony formation assays were performed as follows: 200 cells were plated in six-well plates and subjected to treatment with different concentrations of a specific drug after 1 and 5 days. After an additional 5 days, cells were stained with crystal violet and colonies were counted by eye.

Immunofluorescence

ZL55 cells transfected with BAP1FL or BAP1Δ were fixed for 10 minutes with 4% paraformaldehyde, permeabilized with 0.1% TX-100 for 10 minutes, and blocked with phosphate-buffered saline containing 1% bovine serum albumin and 1% normal goat serum before incubation overnight at 4°C with Bap1 antibody. Alexa Fluor 488 goat anti-mouse (Life Technologies) antibody was then added for 1 hour at room temperature. Coverslips were mounted using Prolong Gold antifade reagent containing 4,6-diamino-2-phenylindole (Life Technologies). Images were acquired using a Leica DM6000 confocal microscope (Leica Biosystems, Nussloch, Germany).

Spheroid Formation and Viability Assay

Spheroid formation assays were performed as previously described.²⁴ At day 4 after seeding, the spheroids were treated with different drugs for 6 days and viability was analyzed using the CellTiter-Glo Luminescent Cell Viability Assay (Promega, Dübendorf, Switzerland) to determine the adenosine triphosphate (ATP) content. Luminescence was acquired by using a GloMax 96 Microplate Luminometer (Promega). Each experiment was performed in triplicate.

Phylogenetic Analysis

Multiple alignments of the protein sequences have been performed through MAFFT FFT-NS-i (v7.215) (<http://mafft>.

cbrc.jp/alignment/server/). A phylogenetic tree was created with Molecular Evolutionary Genetics Analysis software and the following sequences were obtained from the National Center for Biotechnology Information: *Homo sapiens* (reference sequence [ref seq] XM_017007303.1), *Pongo abelii* (ref seq XM_009238935.1), *Mandrillus leucophaeus* (ref seq XM_011986223.1), *Colobus angolensis palliatus* (ref seq XM_011958849.1), *Chlorocebus sabaeus* (ref seq XM_007984488.1), *Rhinopithecus roxellana* (ref seq XM_010365018.1), *Tupaia chinensis* (ref seq XM_006169325.2), *Pteropus vampyrus* (ref seq XM_011372563.1), *Pteropus alecto* (ref seq XM_015593797.1), *Bos taurus* (ref seq NM_001102549.1), *Ovis aries* (ref seq XM_012099955.2), and *Loxodonta africana* (ref seq XM_010589758.1).

Statistical Analysis

Statistical analysis was performed with GraphPad Prism software, version 5.04 (GraphPad Software, La Jolla, CA). Data are presented as the average plus or minus SD. To determine significant additive effects

between combination treatments and inhibition of cell death with the inhibitors, an analysis of variance test was performed. Differences with a *p* value less than 0.05 were considered significant.

Results

Identification and Characterization of a Novel BAP1 Splice Variant

While investigating BAP1 transcripts in MPM cell lines, we identified a shorter variant (BAP1Δ) missing 54 base pairs within exon 9 compared with the full-length BAP1 (BAP1FL) (Fig. 1A). On the basis of data on the crystal structure of the UCH domain (<https://www.ncbi.nlm.nih.gov/Structure/cdd/cddsrv.cgi?ascbin=8&maxaln=10&seltype=2&uid=187738&querygi=508123781&aln=4,10,0,32,42,33,63,106,96,51,157,150,69>), BAP1Δ is missing 12 amino acids of the catalytic region and part of the BARD1 binding domain and has been already listed as BAP1 transcript in the Ensembl database. It may result from a second acceptor site (<http://www.umd.be/HSF3/index.html>), which is almost as strong as the one for

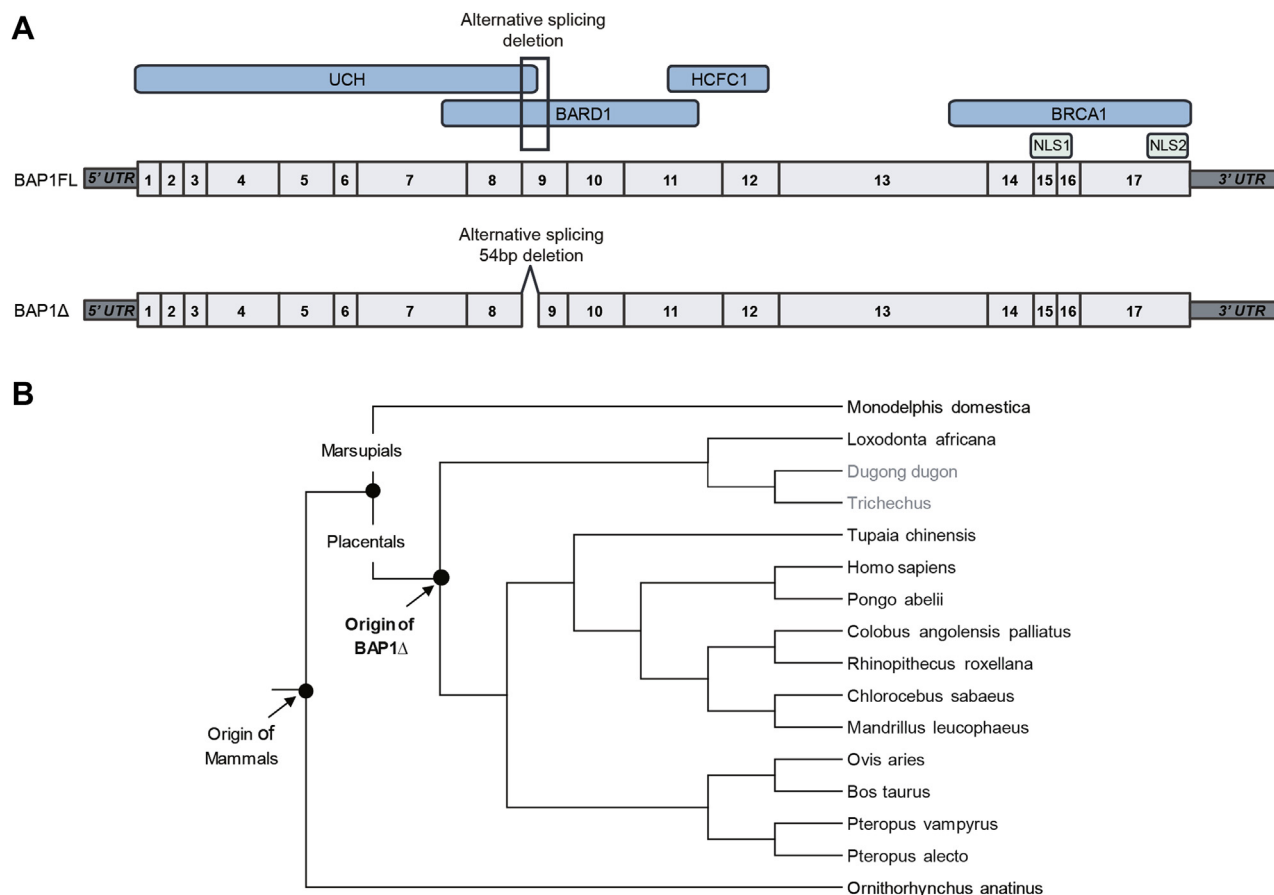


Figure 1. Identification of a novel BRCA associated protein1 (BAP1) splice variant (BAP1Δ). (A) Schematic representation of a coding sequence and protein domains of full-length BAP1 (BAP1FL) and BAP1Δ. (B) Phylogenetic tree of the protein sequences of BAP1Δ. The phylogenetic analysis indicated that the first appearance of BAP1Δ dates back to approximately 150 million of years ago. UCH, ubiquitin carboxyl hydrolase; BARD1, BRCA1 associated RING domain 1; HCFC1, host cell factor C1; BRCA1, BRCA1, DNA repair associated; UTR, untranslated region; NLS, nuclear localization signal; bp, base pair.

BAP1FL. BAP1 Δ is present in several species, and multi-species sequence alignment and phylogeny analysis revealed that BAP1 Δ appeared first in placentals, dating back to approximately 150 million years ago (Fig. 1B and Supplementary Data 1). A fragment covering the region of alternative splicing was amplified by PCR, which revealed the expression of both BAP1FL and BAP1 Δ in MPM (Fig. 2A). Using a set of primers that allows detection of BAP1 Δ specifically, we detected the BAP1 Δ isoform in both MPM cell lines and tumors (Fig. 2B). Interestingly, BAP1 Δ was less abundant in tumors expressing WT BAP1 than in nontumor samples (Fig. 2C).

HEK293 cells transfected with BAP1FL (Fig. 3A) showed a reduction of monoubiquitinated H2A, whereas no change was observed in the cells expressing BAP1 Δ (Fig. 3B and Supplementary Fig. 1), confirming that the deubiquitinase activity of this splice variant is impaired, which is consistent with our prediction based on the sequence. We transfected BAP1-deficient ZL55 mesothelioma cells with BAP1FL or BAP1 Δ ; then, using

immunofluorescence analysis, we determined that BAP1 Δ localizes to the nucleus, however, not to the same extent as BAP1FL (Fig. 3C). This observation was confirmed in experiments in which ZL55 cells stably expressing control vector or pCI-Puro_BAP1FL were transiently transfected with increasing amounts of pCI-Puro_BAP1 Δ , after which cytosolic versus nuclear fractions were isolated. Addition of BAP1 Δ resulted in increased levels of high-molecular-weight bands with BAP1 immunoreactivity in total lysates (Fig. 3D). Quantification of cellular fractionation experiments in single cDNA-expressing cells revealed a 53% plus or minus 4% decrease in nuclear accumulation of BAP1 Δ compared with BAP1FL, as estimated by comparing the percentage of normalized BAP1 immunoreactivity present in the nucleus (Fig. 3E and Supplementary Fig. 1). In cells coexpressing BAP1FL and BAP1 Δ , the quantification of BAP1FL as the sum of molecular forms higher than BAP1 Δ (see Fig. 3E) indicated a shift in BAP1 distribution from nucleus to cytosol (Fig. 3F).

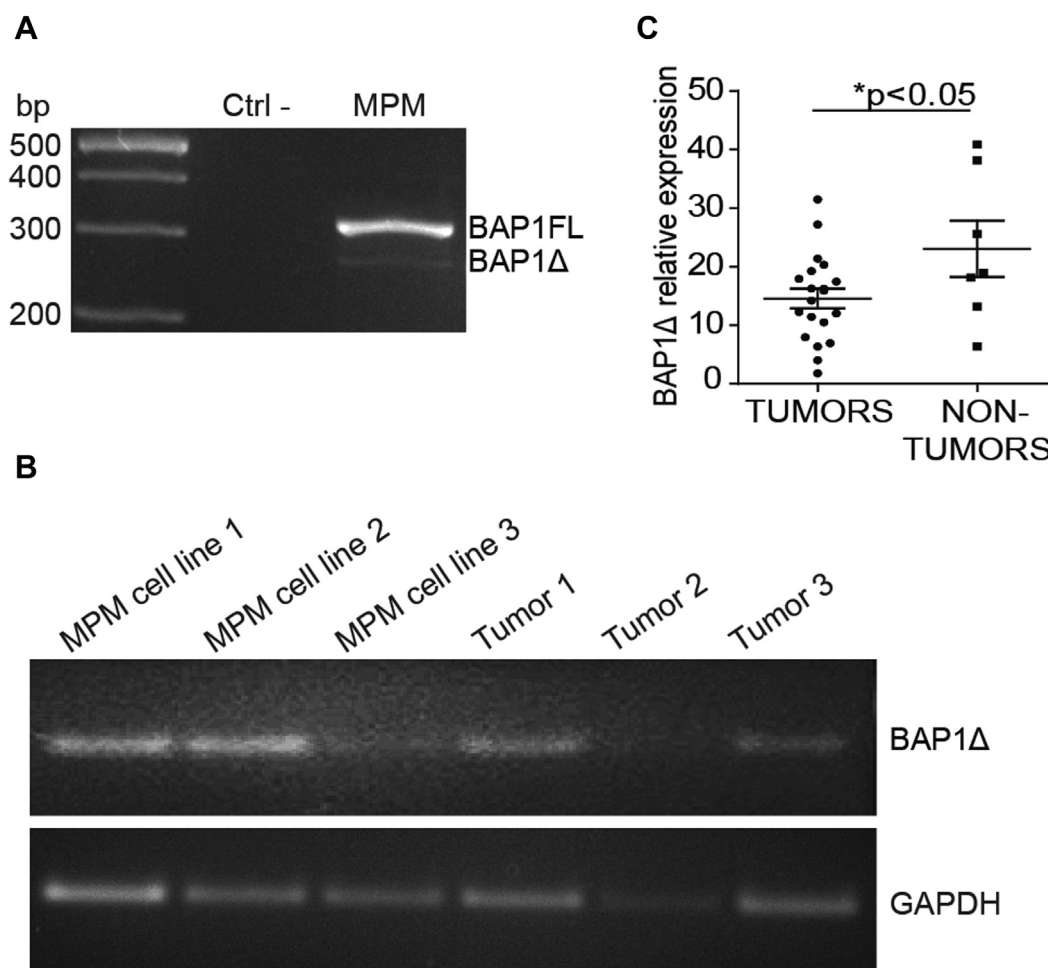


Figure 2. Characterization of BRCA associated protein1 (BAP1) splice variant (BAP1 Δ). Detection of full-length BAP1 (BAP1FL) and BAP1 Δ in a representative malignant pleural mesothelioma (MPM) cell line (A) and different level of BAP1 Δ expression in MPM cell lines and tumor samples (B). (C) Quantitative polymerase chain reaction of BAP1 Δ in wild-type BAP1-expressing tumors and nontumor samples. Ctrl, control; GAPDH, glyceraldehyde-3-phosphate dehydrogenase.

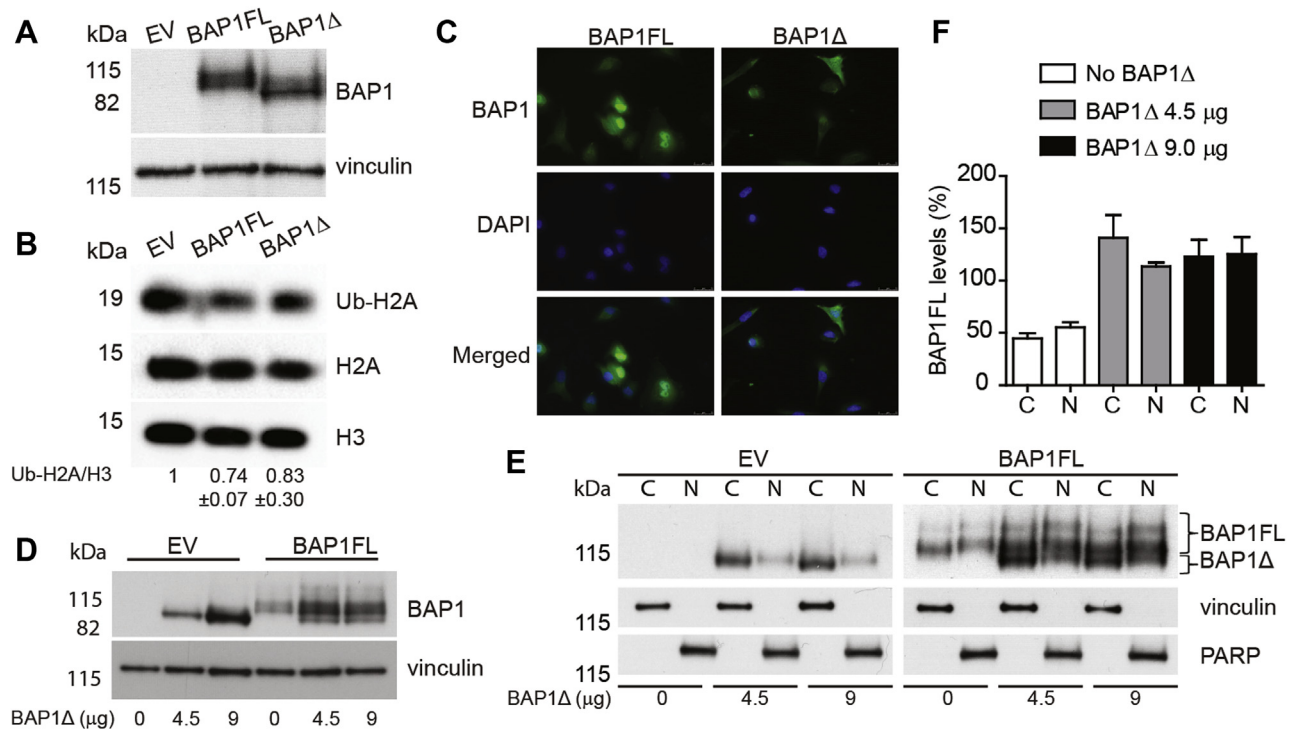


Figure 3. Defective deubiquitinating activity and nuclear localization of BRCA associated protein1 (BAP1) splice variant (BAP1Δ). (A) HEK293 cells were transiently transfected with empty vector (EV) or with full-length BAP1 (BAP1FL) and BAP1Δ cDNA. (B) Core histones were isolated by acidic extraction²⁶ and Western blot was performed to detect monoubiquitination levels of histone H2A (K119Ub-H2A). Results are representative of three independent experiments. (C) ZL55 cells transfected with BAP1FL and BAP1Δ cDNA were analyzed for BAP1 immunoreactivity by immunofluorescence. ZL55 cells expressing EV or BAP1FL were transfected with increasing amounts of BAP1Δ cDNA (D) and BAP1 subcellular distribution was analyzed (E). Parentheses indicate bands considered as BAP1FL and BAP1Δ in the quantification of nuclear versus cytosolic fraction. (F) Quantification of cytosolic and nuclear BAP1FL (including high-molecular-weight forms) in the absence or presence of coexpression of BAP1Δ (n = 3). DAPI, 4,6-diamino-2-phenylindole; C, cytosolic extract; N, nuclear extract; PARP, poly(adenosine diphosphate-ribose) polymerase.

Role of BAP1Δ in MPM Sensitization to PARP Inhibitor

To assess the relevance of BAP1Δ expression in MPM, we used transfected ZL55 cells to assess cell survival after treatment with olaparib, a drug known to be more potent in BAP1-deficient cells.^{11,12} Basal levels of protein poly adenosine diphosphate-ribosylation (PARylation), which is indicative of PARP activity were detected, which was consistent with what had been already observed in glioma spheroids,²⁸ and they decreased after olaparib treatment (Fig. 4A). We could observe a twofold to threefold increase in cytotoxicity of the drug in BAP1Δ-transfected cells compared with in BAP1FL-transfected cells in both clonogenic (Fig. 4B) and spheroid viability assays (Fig. 4C).

Both Levels of BAP1Δ and GDC0980-Mediated BRCA1 Depletion Sensitize to Olaparib

Inhibition of PARP is an established therapeutic strategy for breast and ovarian cancer in BRCA1-deficient tumors.²⁹ As expected,³⁰ we observed an increased

phosphorylation of histone H2AX, a known marker of DNA DSBs, upon treatment with olaparib in MPM spheroids (Supplementary Fig. 2), suggesting engagement of BRCA1 in DNA repair.^{31,32} Because BAP1 can interact with BRCA1 and because BAP1FL reconstitution in BAP1-null cell lines leads to resistance to PARP inhibition (unlike in BAP1Δ-reconstituted cells), we analyzed the expression of BAP1Δ compared with expression of BAP1FL in MPM cell lines. Sequencing revealed the presence of WT BAP1 in all tested cell lines. We grouped them in two groups: low BAP1Δ, with a BAP1Δ/BAP1 expression ratio value of 20% or less (Mero82, ACC-Meso1, SDM103T2, H2052) and high BAP1Δ (BAP1Δ^{high}), with a BAP1Δ/BAP1 expression ratio value greater than 20% (MSTO-211H, SPC111, ZL34, and Mero41) (Fig. 5A). The threshold value of 20% represents the median of BAP1Δ/BAP1 in the MPM cell lines. We then tested whether BRCA1 depletion mediated by phosphoinositide 3-kinase (PI3K) pathway inhibition³³ would sensitize MPM cells to PARP inhibition in MPM cell lines able to form spheroids. Spheroids were treated individually with olaparib or in combination with

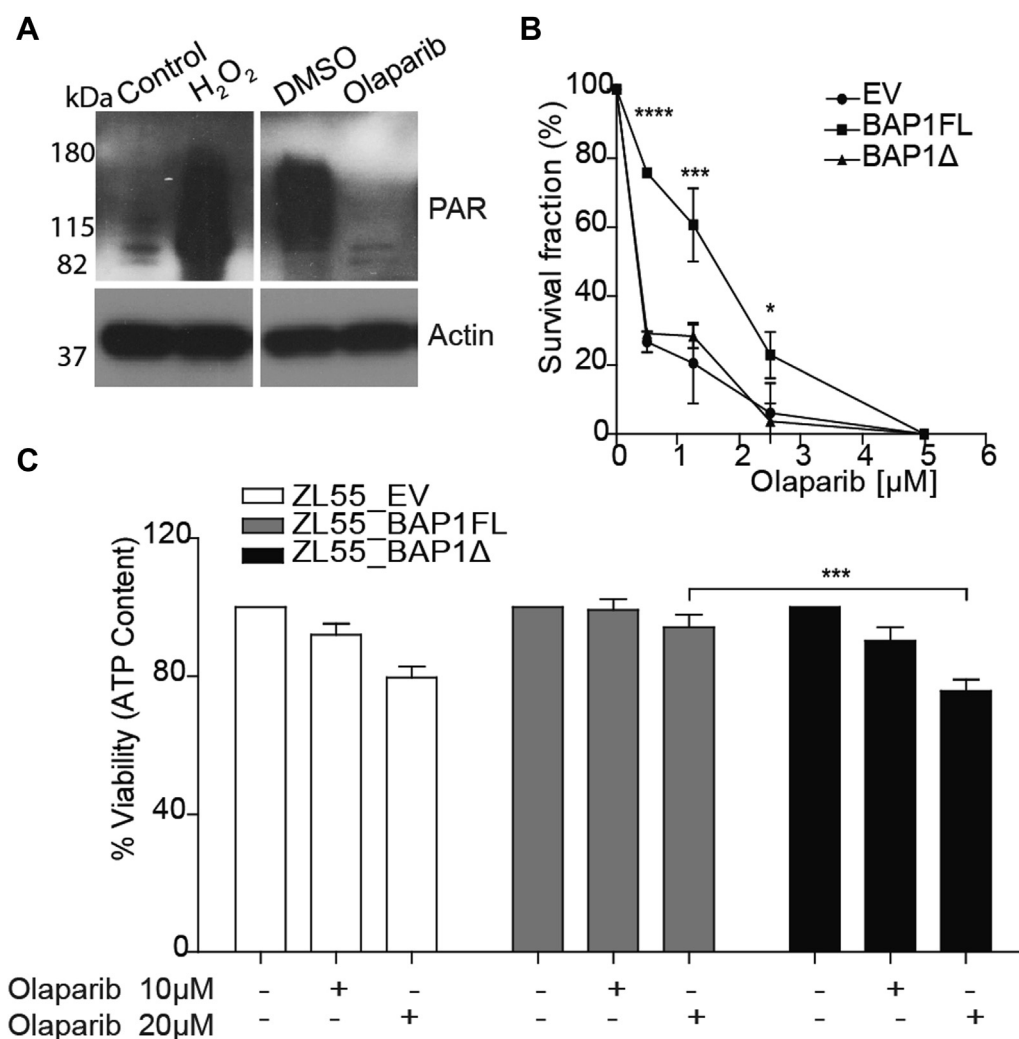


Figure 4. BRCA associated protein1 (BAP1) splice variant (BAP1Δ) sensitizes malignant pleural mesothelioma cells to olaparib in two- and three-dimensional in vitro cell survival assays. (A) Olaparib decreased poly adenosine diphosphate-ribosylation in spheroids. H₂O₂-induced activation of PARP1 resulting in poly adenosine diphosphate-ribosylation of proteins served as a positive control for poly(adenosine diphosphate-ribose) (PAR) immunoblot. Cells expressing BAP1Δ were as sensitive as BAP1-deficient cells to olaparib in two- (B) and three-dimensional (C) models. Results derived from three independent experiments performed in triplicate. **p* < 0.05; ****p* < 0.001; *****p* < 0.0001. EV, empty vector; BAP1FL, full-length BAP1; ATP, adenosine triphosphate.

GDC0980, a dual PI3K-mammalian target of rapamycin (mTOR) inhibitor. As expected, phosphorylated protein S6 (downstream effector of PI3K-mTOR pathway) levels decreased after GDC0980 treatment in spheroids, as we had previously observed in two-dimensional models²⁴ (Fig. 5B). BRCA1 expression was reduced as expected after GDC0980 treatment in the two cell lines representing the low BAP1Δ and BAP1Δ^{high} groups selected on the basis of similar total BAP1 levels. Moreover, BRCA1 downregulation was intensified in the BAP1Δ^{high} cell line SPC111 when treated with the combined treatment (Fig. 5C). BAP1Δ/BAP1 high ratio sensitized MPM cell lines to olaparib (Fig. 5D and E). As previously shown, GDC0980 decreased ATP content²⁴ and the BAP1Δ^{high} group showed a complete ATP drop with the combined

treatment (see Fig. 5E). Spheroids derived from the normal mesothelium cell line SDM104 were resistant to olaparib and, as previously described, were growth inhibited by GDC0980.²⁴ ATP content decreased further by the combined treatment, albeit to a lesser extent compared with mesothelioma cells (see Fig. 5E).

Discussion

In this study we showed that expression of the BAP1Δ isoform over a threshold level, defined as 20% of total BAP1, sensitizes MPM cells expressing WT BAP1 to olaparib-induced cytotoxicity. Combining this treatment with PI3K-mTOR inhibitors, which decrease BRCA1 levels, results in stronger effects.

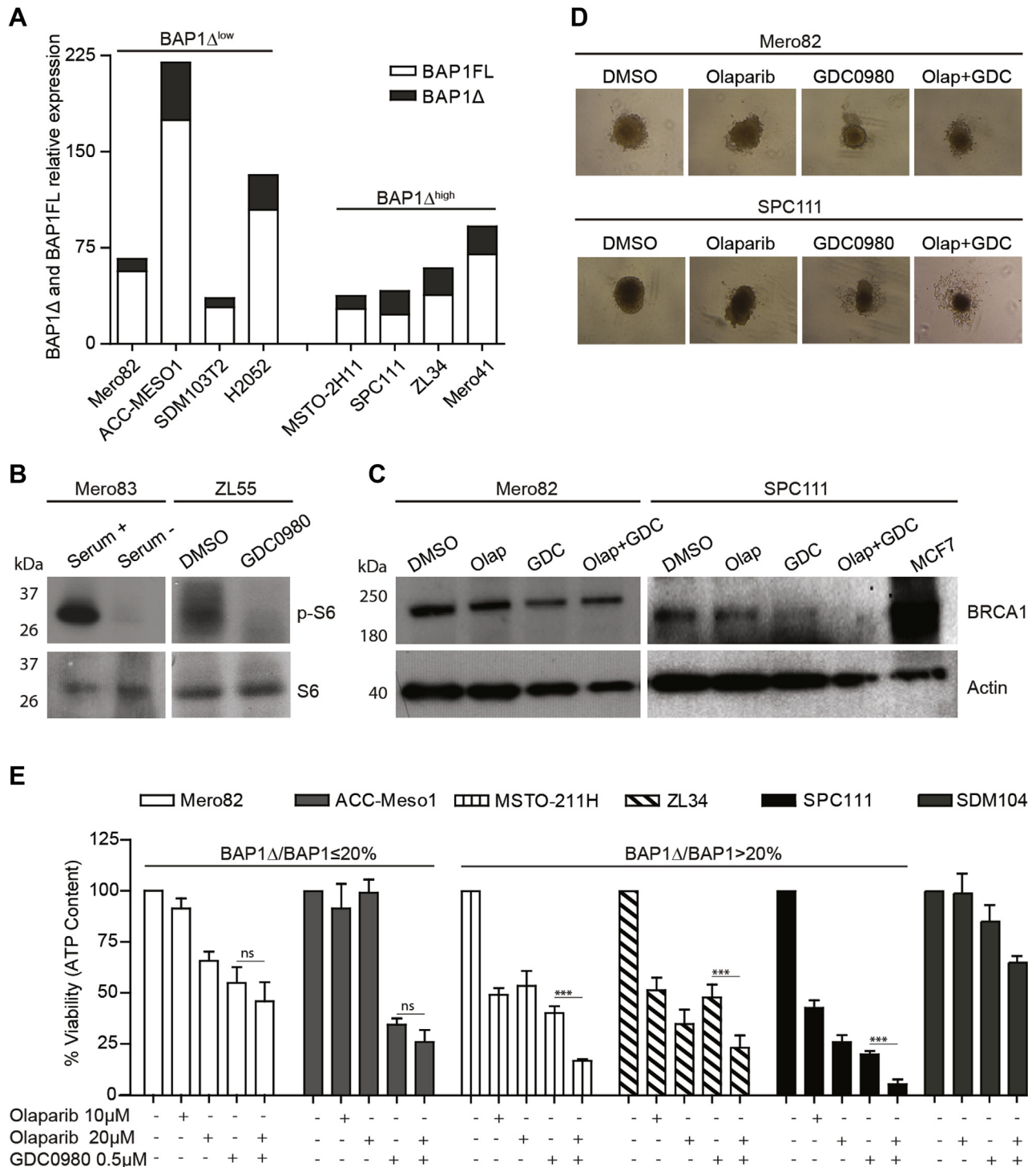


Figure 5. BRCA associated protein1 (BAP1) splice variant (BAP1Δ) expression level and inhibition of phosphoinositide 3-kinase-mammalian target of rapamycin sensitize malignant pleural mesothelioma (MPM) cells to olaparib. (A) Relative expression of BAP1Δ and full-length BAP1 (BAP1FL) in MPM. (B) GDC0980 decreased phosphorylation of protein S6 (p-S6) in MPM spheroids. (C) BRCA1 levels in three-dimensional spheroids obtained from Mero8p-s62 and SPC111 cells untreated (DMSO) and treated with 20μM olaparib or 0.5 μM GDC0980 individually or in combination. MCF7 cells lysate was included as positive control for BRCA1 expression. (D) Representative light micrographs of Mero-82 and SPC111 spheroids treated with 20 μM olaparib and 0.5 μM GDC0980. (E) Effect of combined olaparib and GDC-0980 in MPM cell lines grouped on the basis of high (BAP1Δ^{high}) and low (BAP1Δ^{low}) expression of BAP1Δ or in normal mesothelial cells SDM104. Results derived from three independent experiments performed in triplicate. ****p* < 0.001. BAP1FL, full-length BAP1.

Deficiency in processes involved in DNA damage response can be exploited as a therapeutic strategy. For example, when DNA single-strand breaks occur, cells undergo PARP-mediated DNA repair. If this mechanism is inhibited (e.g., by olaparib), single-strand breaks persist and turn into DSBs. When these accumulate, they become lethal for cancer cells when specific DNA repair processes (such as homologous recombination) are impaired, as in the case of BRCA-deficient breast and ovarian cancer.²⁹ Interestingly, the expression of BRCA1 is essential in mediating apoptosis induced by vinorelbine (an antimitotic drug used in second-line therapy) in MPM cells,³⁴ and low BRCA-1 expression and vinorelbine resistance were observed in about 40% of patients with MPM. However, it remains unclear whether this is due to BAP1 loss of function (especially because recent studies have suggested a role of BAP1 in BRCA1 stabilization in mesothelioma³⁵) or to some other mechanism in which BAP1Δ might be involved. Homologous recombination deficiency can also be induced by impairing BRCA1 expression through PI3K inhibition, resulting in cell sensitization to PARP inhibition.³³

In our study we characterized a novel isoform of BAP1 that exhibits diminished deubiquitinating activity on histone H2A and is very likely unable to exert its function in DNA repair. The association between alternative splicing and cancer is rapidly emerging, because isoforms of a protein can have opposite functions.³⁶ The appearance of this isoform in placentals may reflect functional requirements unique to placental mammals, as is the case for other chromatin modifiers.³⁷ Interestingly, the alternative acceptor site for BAP1Δ scores almost as high as the one for BAP1FL, and therefore, exonic splicing enhancers³⁸ may possibly play a role in the differential expression. BAP1Δ was still able to enter the nucleus; therefore, a possible mechanism of action is interference with BAP1FL dimerization with ASLX1³⁹ and consequent inactivation. Another intriguing possibility is inferred by the appearance of higher-molecular-weight forms of BAP1 after coexpression of BAP1FL and BAP1Δ. The higher molecular weight may represent ubiquitin conjugating enzyme E2 O-dependent ubiquitin-conjugated forms of BAP1, which accumulate especially when BAP1 cannot efficiently deubiquitinate itself.⁴⁰

Although further investigations that are beyond the scope of this study are necessary to elucidate the underlying mechanism of BAP1Δ interference with BAP1FL, we have demonstrated that expression of BAP1Δ over a certain threshold level, even in the presence of functional BAP1, could be exploited in combination with PI3K-mTOR inhibitors in a therapeutic approach using PARP inhibitors.

Potential synthetic lethality between PARP and PI3K/mTOR inhibition has been recently documented in

several models,^{33,41–43} and besides decreasing BRCA1 expression, other mechanisms involve nucleotide depletion.⁴¹ Olaparib is a U.S. Food and Drug Administration–approved targeted therapy in cancer,²⁹ and GDC0980 has proved to have some efficacy in a clinical study, especially in patients with mesothelioma⁴⁴; therefore, this strategy is potentially easy to implement in a clinical trial. Because BAP1 is WT in 77% of MPMs,⁴⁵ 15% of patients with MPM could potentially benefit from this therapeutic strategy.

Acknowledgments

This work was supported by the Walter Bruckerhoff Foundation, Swiss National Science Foundation grant CRSII3 147697/1, and the Foundation for Applied Cancer Research.

Supplementary Data

Note: To access the supplementary material accompanying this article, visit the online version of the *Journal of Thoracic Oncology* at www.jto.org and at <http://dx.doi.org/10.1016/j.jtho.2017.03.023>.

References

- Guo G, Chmielecki J, Goparaju C, et al. Whole-exome sequencing reveals frequent genetic alterations in BAP1, NF2, CDKN2A, and CUL1 in malignant pleural mesothelioma. *Cancer Res*. 2015;75:264–269.
- Xu J, Kadariya Y, Cheung M, et al. Germline mutation of Bap1 accelerates development of asbestos-induced malignant mesothelioma. *Cancer Res*. 2014;74:4388–4397.
- Bott M, Brevet M, Taylor BS, et al. The nuclear deubiquitinase BAP1 is commonly inactivated by somatic mutations and 3p21.1 losses in malignant pleural mesothelioma. *Nat Genet*. 2011;43:668–672.
- Napolitano A, Pellegrini L, Dey A, et al. Minimal asbestos exposure in germline BAP1 heterozygous mice is associated with deregulated inflammatory response and increased risk of mesothelioma. *Oncogene*. 2016;35:1996–2002.
- Testa JR, Cheung M, Pei J, et al. Germline BAP1 mutations predispose to malignant mesothelioma. *Nat Genet*. 2011;43:1022–1025.
- Jensen DE, Proctor M, Marquis ST, et al. BAP1: a novel ubiquitin hydrolase which binds to the BRCA1 RING finger and enhances BRCA1-mediated cell growth suppression. *Oncogene*. 1998;16:1097–1112.
- Nishikawa H, Wu W, Koike A, et al. BRCA1-associated protein 1 interferes with BRCA1/BARD1 RING heterodimer activity. *Cancer Res*. 2009;69:111–119.
- Narod SA, Foulkes WD. BRCA1 and BRCA2: 1994 and beyond. *Nat Rev Cancer*. 2004;4:665–676.
- Ventii KH, Devi NS, Friedrich KL, et al. BRCA1-associated protein-1 is a tumor suppressor that requires deubiquitinating activity and nuclear localization. *Cancer Res*. 2008;68:6953–6962.

10. Scheuermann JC, de Ayala Alonso AG, Oktaba K, et al. Histone H2A deubiquitinase activity of the polycomb repressive complex PR-DUB. *Nature*. 2010;465:243-247.
11. Pena-Llopis S, Vega-Rubin-de-Celis S, Liao A, et al. BAP1 loss defines a new class of renal cell carcinoma. *Nat Genet*. 2012;44:751-759.
12. Yu H, Pak H, Hammond-Martel I, et al. Tumor suppressor and deubiquitinase BAP1 promotes DNA double-strand break repair. *Proc Natl Acad Sci U S A*. 2014;111:285-290.
13. Paronetto MP, Passacantilli I, Sette C. Alternative splicing and cell survival: from tissue homeostasis to disease. *Cell Death Differ*. 2016;23:1919-1929.
14. Thurneysen C, Opitz I, Kurtz S, Weder W, Stahal RA, Felley-Bosco E. Functional inactivation of NF2/merlin in human mesothelioma. *Lung Cancer*. 2009;64:140-147.
15. Bianchi AB, Mitsunaga SI, Cheng JQ, et al. High frequency of inactivating mutations in the neurofibromatosis type 2 gene (NF2) in primary malignant mesotheliomas. *Proc Natl Acad Sci U S A*. 1995;92:10854-10858.
16. Sekido Y, Pass HI, Bader S, et al. Neurofibromatosis type 2 (NF2) gene is somatically mutated in mesothelioma but not in lung cancer. *Cancer Res*. 1995;55:1227-1231.
17. Deguen B, Goutebroze L, Giovannini M, et al. Heterogeneity of mesothelioma cell lines as defined by altered genomic structure and expression of the NF2 gene. *Int J Cancer*. 1998;77:554-560.
18. Fleury-Feith J, Lecomte C, Renier A, et al. Hemizygosity of Nf2 is associated with increased susceptibility to asbestos-induced peritoneal tumours. *Oncogene*. 2003;22:3799-3805.
19. Jongma J, van Montfort E, Vooijs M, et al. A conditional mouse model for malignant mesothelioma. *Cancer Cell*. 2008;13:261-271.
20. Chang LS, Akhmametyeva EM, Wu Y, Zhu L, Welling DB. Multiple transcription initiation sites, alternative splicing, and differential polyadenylation contribute to the complexity of human neurofibromatosis 2 transcripts. *Genomics*. 2002;79:63-76.
21. Sherman L, Xu HM, Geist RT, et al. Interdomain binding mediates tumor growth suppression by the NF2 gene product. *Oncogene*. 1997;15:2505-2509.
22. Gutmann DH, Geist RT, Xu HM, Kim JS, Saporito-Irwin S. Defects in neurofibromatosis 2 protein function can arise at multiple levels. *Hum Mol Genet*. 1998;7:335-345.
23. Giovannini M, Robanus-Maandag E, Niwa-Kawakita M, et al. Schwann cell hyperplasia and tumors in transgenic mice expressing a naturally occurring mutant NF2 protein. *Genes Dev*. 1999;13:978-986.
24. Echeverry N, Ziltener G, Barbone D, et al. Inhibition of autophagy sensitizes malignant pleural mesothelioma cells to dual PI3K/mTOR inhibitors. *Cell Death Dis*. 2015;6:e1757.
25. Renganathan A, Kresoja-Rakic J, Echeverry N, et al. GAS5 long non-coding RNA in malignant pleural mesothelioma. *Mol Cancer*. 2014;13:119.
26. Pinato S, Scandiuzzi C, Arnaudo N, Citterio E, Gaudino G, Penengo L. RNF168, a new RING finger, MIU-containing protein that modifies chromatin by ubiquitination of histones H2A and H2AX. *BMC Mol Biol*. 2009;10:55.
27. Andre M, Latado H, Felley-Bosco E. Inducible nitric oxide synthase-dependent stimulation of PKGI and phosphorylation of VASP in human embryonic kidney cells. *Biochem Pharmacol*. 2005;69:595-602.
28. Wharton SB, McNelis U, Bell HS, Whittle IR. Expression of poly(ADP-ribose) polymerase and distribution of poly(ADP-ribose) polymerase in glioblastoma and in a glioma multicellular tumour spheroid model. *Neuropathol Appl Neurobiol*. 2000;26:528-535.
29. Weil MK, Chen AP. PARP inhibitor treatment in ovarian and breast cancer. *Curr Probl Cancer*. 2011;35:7-50.
30. Bryant HE, Schultz N, Thomas HD, et al. Specific killing of BRCA2-deficient tumours with inhibitors of poly(ADP-ribose) polymerase. *Nature*. 2005;434:913-917.
31. Saleh-Gohari N, Bryant HE, Schultz N, Parker KM, Cassel TN, Helleday T. Spontaneous homologous recombination is induced by collapsed replication forks that are caused by endogenous DNA single-strand breaks. *Mol Cell Biol*. 2005;25:7158-7169.
32. Arnaudeau C, Lundin C, Helleday T. DNA double-strand breaks associated with replication forks are predominantly repaired by homologous recombination involving an exchange mechanism in mammalian cells. *J Mol Biol*. 2001;307:1235-1245.
33. Ibrahim YH, Garcia-Garcia C, Serra V, et al. PI3K inhibition impairs BRCA1/2 expression and sensitizes BRCA-proficient triple-negative breast cancer to PARP inhibition. *Cancer Discov*. 2012;2:1036-1047.
34. Busacca S, Sheaff M, Arthur K, et al. BRCA1 is an essential mediator of vinorelbine-induced apoptosis in mesothelioma. *J Pathol*. 2012;227:200-208.
35. Hakiri S, Osada H, Ishiguro F, et al. Functional differences between wild-type and mutant-type BAP1 tumor suppressor against malignant mesothelioma cells. *Cancer Sci*. 2015.
36. Oltean S, Bates DO. Hallmarks of alternative splicing in cancer. *Oncogene*. 2014;33:5311-5318.
37. Privalsky ML, Snyder CA, Goodson ML. Corepressor diversification by alternative mRNA splicing is species specific. *BMC Evol Biol*. 2016;16:221.
38. Lee Y, Rio DC. Mechanisms and regulation of alternative pre-mRNA splicing. *Annu Rev Biochem*. 2015;84:291-323.
39. Sahtoe DD, van Dijk WJ, Ekkebus R, Ovaa H, Sixma TK. BAP1/ASXL1 recruitment and activation for H2A deubiquitination. *Nat Commun*. 2016;7:10292.
40. Mashtalir N, Daou S, Barbour H, et al. Autodeubiquitination protects the tumor suppressor BAP1 from cytoplasmic sequestration mediated by the atypical ubiquitin ligase UBE2O. *Mol Cell*. 2014;54:392-406.
41. Juvekar A, Hu H, Yadegarynia S, et al. Phosphoinositide 3-kinase inhibitors induce DNA damage through nucleoside depletion. *Proc Natl Acad Sci U S A*. 2016;113:E4338-E4347.
42. Juvekar A, Burgal LN, Hu H, et al. Combining a PI3K inhibitor with a PARP inhibitor provides an effective therapy for BRCA1-related breast cancer. *Cancer Discov*. 2012;2:1048-1063.
43. De P, Sun Y, Carlson JH, Friedman LS, Leyland-Jones BR, Dey N. Doubling down on the PI3K-AKT-mTOR pathway

■■■ 2017

BAP1 Isoform Affects Mesothelioma Response 11

- enhances the antitumor efficacy of PARP inhibitor in triple negative breast cancer model beyond BRCA-mutated. *Neoplasia*. 2014;16:43-72.
44. Dolly SO, Wagner AJ, Bendell JC, et al. Phase I study of apitolisib (GDC-0980), dual phosphatidylinositol-3-kinase and mammalian target of rapamycin kinase inhibitor, in patients with advanced solid tumors. *Clin Cancer Res*. 2016;22:2874-2884.
45. Bueno R, Stawiski EW, Goldstein LD, et al. Comprehensive genomic analysis of malignant pleural mesothelioma identifies recurrent mutations, gene fusions and splicing alterations. *Nat Genet*. 2016;48:407-416.